Surface Effects on Capped and Uncapped Nanocrystals

Garnett W. Bryant*

Atomic Physics Division, National Institute of Standards and Technology, Gaithersburg, Maryland 20899-8423

W. Jaskolski

Instytut Fizyki, UMK, Grudziadzka 5, 87-100 Torun, Poland

Received: June 29, 2005; In Final Form: August 24, 2005

Surface effects significantly influence the functionality of semiconductor nanocrystals. A theoretical understanding of these effects requires an atomic-scale description of the surface. We present an atomistic tight-binding theory of the electronic and optical properties of passivated and unpassivated CdS nanocrystals and CdS/ZnS core/shell nanocrystals. Fully passivated dots, with all dangling bonds saturated, have no surface states in the fundamental band gap, and all near-band-edge states are quantum-confined internal states. When surface anion dangling bonds are unpassivated, an anion-derived, narrow (bandwidth 0.05 eV), surface-state band lies 0.5 eV above the valence band edge, and a broader (0.2 eV) band of back-bonded surface states exists in the gap just above the valence band edge. When surface cation dangling bonds are unpassivated, a broad band of mixed surface/internal states exists above the conduction band edge. Partial passivation can push internal levels above the internal levels of a fully passivated dot or into the band gap. Because of this sensitivity to passivation, explicit models for surface effects are needed to describe accurately internal states. Capping the CdS dot with ZnS reduces the effect of the surface on the internal electronic states and optical properties. Six monolayers of ZnS are needed to eliminate the influence of any surface states on the internal states.

1. Introduction

Semiconductor quantum dots and nanocrystals have been studied intensely due to their enticing possibilities as artificial atoms with enhanced optical properties. Nanocrystals are being used as building blocks for bio/nanohybrids, for use in biological systems as biomarkers[1−4] and resonant energy-transfer sensors,[5−7] and in nano/molecular assemblies.[8−12] Construction of these bio/nanohybrids and nano/molecular assemblies is a challenging, ongoing problem. An understanding of how dots function in these structures is needed so that tailored nanooptics with these systems can be exploited. Surface effects significantly influence the functionality of bare nanocrystals as well as that of passivated or conjugated nanocrystals. Passivation with ligands or high band-gap semiconductor shells is necessary to reduce surface trap densities, enhance quantum yield, and increase photostability,[13−18] while conjugation with various molecules is needed to provide selectivity for biological and chemical sensing and to build the connections for nano/molecular assemblies.

Both continuum and atomistic theories have been used to understand quantum dots. Continuum effective-mass theory[19−23] can provide an understanding of internal confined states in semiconductor nanocrystals, although atomistic theories are needed for a more complete understanding of these confined states.[24−31] To describe surface states, continuum models have been developed with generalized boundary conditions that allow for states that do not vanish at the nanocrystal boundary.[32] However, there is no direct way to clearly model surface effects with such continuum theories, because the atomic detail of the surface is still ignored. A full theoretical understanding of surface effects requires atomistic models capable of describing surface faceting and relaxation, site-dependent partial and random passivation, the molecular structure of passivants, and few-monolayer shells. These effects cannot be treated by effective-mass theories. Here, we present an atomistic tight-binding theory of the electronic structure and optical properties of passivated, unpassivated, and core/shell nanocrystals to study these surface effects. Most importantly, we study the effectiveness of passivating a core nanocrystal with a capping layer by determining the shell thickness needed to eliminate fully the effect of surface traps on the core nanocrystal optical response. Ideally, the capping layer should be grown thick enough that none of the surface states couples to the internal states confined in the core. Use of a high band-gap cap further ensures that the states confined in the core cannot leak to the surface. Finally, a cap that provides type I band alignment with a barrier for both electrons and holes ensures that both electrons and holes remain confined to the core and give spatially direct transitions. ZnS is a typical capping layer for nanocrystals such as CdSe and CdS that satisfies these criteria.[13−18] In practice, the thickness of the cap that should be grown is determined by the lattice mismatch between core and cap. Caps that are too thick develop dislocations to relieve strain.[15] These dislocations can degrade the optical response.

2. Tight-Binding Theory

We calculate electron and hole states in nanocrystals by use of the empirical tight-binding (ETB) method.[25−31] The ETB approach is an atomistic approach well-suited for calculating the electronic states of nanosystems with atomic-scale interfaces,

* Corresponding author. E-mail: garnett.bryant@nist.gov.

10.1021/jp0535543 CCC: $30.25
Published on Web 10/01/2005

surface structure, and variations in composition and shape. In this paper, we consider zinc blende, CdS, and CdS/ZnS nanocrystals. We assume that all atoms occupy a common, zinc blende lattice with no relaxation in the bulk, at interfaces, or surfaces. To date, lattice relaxation and surface reconstruction have been considered only for very small nanocrystals with a few hundred atoms.[33−37] Here, we consider a full range of nanocrystal sizes, including core/shell structures with up to 25000 atoms. It is extremely time-consuming to include lattice relaxation and surface reconstruction for the full range of sizes that we consider. For that reason, we limit our attention to unrelaxed structures. Here, we consider spherical nanoparticles.

In our ETB model, each atom is described by its outer valence s orbital, the three outer p orbitals, and a fictitious excited s* orbital, included to mimic the effects of higher-lying states.[38] The empirical Hamiltonians are determined by adjusting the matrix elements to reproduce band gaps and effective masses of the bulk band structures. We include on-site and nearest-neighbor coupling between orbitals. Spin-orbit coupling is included in the theory, but it will not be considered for the results presented here. This simplification allows us to focus on how the spatial trapping at surfaces influences the nanocrystal optical response and how surface effects are suppressed in core/shell structures. For CdS and ZnS, spin-orbit coupling is small (about 80 meV)[39] and should produce a fine-scale splitting of surface states in addition to the effects discussed here.

The electron and hole eigenstates close to the band edges are found by diagonalizing the Hamiltonians with an iterative eigenvalue solver using the Arnoldi method. The nanosystems have on the order of 200−25000 atoms. Typically, we find up to several hundred states closest to the band edge plus all states in the gap. For the largerst nanocrystals considered, this may include about a thousand gap states. In this paper, we consider four simple models for the surface passivation: a surface with all dangling bonds unpassivated, with only cation dangling bonds passivated, with only anion dangling bonds passivated, and with all surface dangling bonds passivated. Complete passivation is modeled by shifting the energy of the dangling bonds, V_{db}, so that all gap states are shifted well above or below the other bands, leaving only internal confined states near the band gap. Complete passivation is achieved for large $|V_{db}|$. The same approach has been used previously.[29,30,40] Partial passivation can also be modeled by a partial shift of the dangling-bond energy. Unpassivated dots are modeled for $V_{db} = 0$.These simple models allow us to assess the general impact of surface passivation and the effect of a capping shell, assessing the full range of passivation with one model parameter, without explicitly modeling a particular passivant. Detailed calculations for a specific passivant would require specifc TB models for that passivant. That is not the purpose of this study. We model CdS and CdS/ZnS nanocrystals with the CdS and ZnS ETB parameters taken from Lippens and Lannoo.[25] We have used this TB model and related TB models to describe successfully ZnS/CdS/ZnS[29] and CdS/HgS/CdS[30] quantum-dot quantum-well nanocrystals. We find that different choices of TB parameters that produce the same bulk band structure typically make small shifts (on the order of 10 meV) in the electronic structure. These shifts would affect fine-scale detail but not influence the robustness of the general features of the electronic structure and optical response that we discuss. We use bulk TB parameters. These parameters could be different near a surface. Again we expect that such differences would affect the fine-scale detail.

Optical spectra are calculated by evaluating the dipole matrix elements for electron and hole eigenstates found in the ETB calculations.[27,28,30] To calculate the spectra, we assume that all anion-derived surface states, due to any unpassivated anion dangling bonds, are occupied and that all cation-derived surface states are empty. In the ETB approach, the matrix elements of the Hamiltonian are determined empirically. However, the local dipole matrix elements needed to calculate spectra are not used explicitly to define the empirical Hamiltonian, so the local dipole matrix elements must be found separately. We find on-site dipole matrix elements by use of calculated atomic dipole matrix elements.[41] Dipole matrix elements between bonding orbitals on nearest-neighbor sites are chosen by reasonable estimates. The qualitative structure in the calculated spectra is insensitive to variations in the dipole matrix elements for bond orbitals for choices of these matrix elements less than the bond length. This shows that allowed transitions are determined by symmetry considerations. We also ignore excitonic effects[27,28,42] on the spectra for the calculations presented here. Including excitonic effects would be computationally very expensive, because we include contributions from all of the gap states.

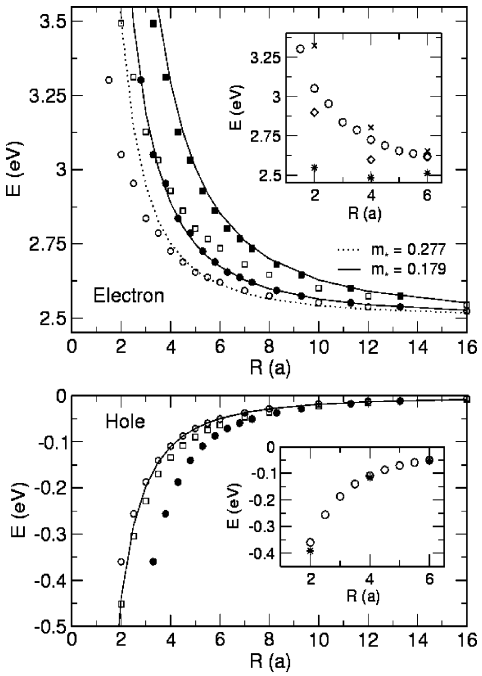

Figure 1. Size dependence of the lowest two (open circles and squares) single-particle electron and hole energy levels E in a CdS nanocrystal (radius R, lattice constant a) with fully passivated dangling bonds calculated with the TB model. The solid curves show the size dependence obtained from an infinite-barrier effective-mass model using the bulk band-edge mass. The dotted curve is a "best" eyeball $1/R^2$ fit. The positions of the TB energy levels shifted to higher R by $1.3a$ are shown as filled circles and squares. The insets compare the position for the lowest level (open circles) in the fully passivated nanocrystal with the level for $R = 2a$, $4a$, and $6a$ when all the dangling bonds are unpassivated (diamonds), only Cd dangling bonds are passivated (filled circles), and only S dangling bonds are passivated (x).

3. Results

A. Surface Effects in Fully Passivated Dots. To illustrate the importance of using an atomistic model to describe surface effects, we first determine the size dependence of the lowest electron and hole states in spherical CdS nanocrystals. We consider the case where all dangling bonds are fully passivated so that there are no gap states localized to the surface, only the quantum-confined internal states. The first two electron and hole levels found with the TB are shown in Figure 1. The energies found with an effective mass model using an infinite barrier

and the bulk effective mass are shown for comparison. The results agree well at large radius R, but the discrepancy increases significantly for decreasing R. A "best" eyeball fit to a $1/R^2$ dependence can be obtained by using a heavier effective mass, as would be appropriate for states away from the band edge. However, for the first two electron levels, a much better fit between the TB results and the results obtained with the infinite-barrier, effective-mass model with the band-edge mass can be obtained simply by shifting the TB results to higher R by $1.3a$, where a is a lattice constant. This indicates that the effective-mass model can provide a reasonable description of the size dependence for radii from $16a$ (10 nm) down to $2a$ (1 nm), provided that the radius used in the effective-mass model is $1.3a$ larger than the physical radius for the nanocrystal. This shows that the electron density is finite on the surface atoms, even when the dangling bonds are fully saturated. The infinite-barrier model can model this finite surface density only by using a larger effective radius. Holes have higher effective mass and lower surface probability than electron levels. A shift of the hole levels to higher R by $1.3a$ significantly worsens the comparison between the TB results and the infinite-barrier, effective-mass results. For holes, the effective radius is nearly the same as the physical radius. The effective-radius model should work well for the lowest electron and hole states in wide band-gap nanocrystals that can be constructed from a single band of bulk zone-center states. In this case, the effective-radius model ensures that the appropriate boundary conditions are applied to the effective-mass model to give the correct state density at the surface. However, as nanocrystal size or band gap decreases, the discrepancies between effective-mass models and tight-binding theory increase due to increased band mixing or hybridization with states away from the zone center, and the effective-radius model should not be enough to remove the discrepancies.

A proper estimation of the effective radius for the effective-mass model requires the use of an atomistic model for the surface. While this effective radius may be interesting as a tool to aid phenomenological modeling, it has limited general utility. It is different for electrons and holes. It is probably different for higher levels (although we have not checked this). More importantly, it loses its utility when other surface passivations are considered. The insets in Figure 1 show the variation of the energy of the first internal confined state for different surface passivations for several values of R. For nanocrystals with unpassivated surface dangling bonds and nanocrystals with unpassivated Cd dangling bonds, the lowest internal electron level does not even depend monotonically on R. Moreover, when the Cd dangling bonds are unsaturated, the electron level can lie below the bulk band edge (2.5 eV). None of these results can come from an effective-mass, infinite-barrier model, even with the use of an effective radius.

B. Dependence on Dangling-Bond Energy. The use of a dangling-bond energy shift V_{db} to model the effects of passivation gives correctly the limit of unpassivated dangling bonds ($V_{db} = 0$) and the limit of fully passivated bonds that produce no gap states ($|V_{db}| \gg 0$). To test the effects of partial passivation, we treat V_{db} as a parameter that can be interpolated between the limit of full passivation and the limit of unpassivated bonds. Here we consider the case of a spherical CdS nanocrystal, radius $R = 4a$, with all cation dangling bonds fully passivated and test the effects of partially passivated S dangling bonds by varying the S dangling-bond energy shift $V_{surf,a}$ (we assume that all S dangling bonds have the same $V_{surf,a}$). The effect on the lowest confined internal electron and hole states is shown in Figures 2 and 3. Analogous results are obtained when we consider the complementary case with the S dangling bonds fully passivated and the Cd dangling bonds partially passivated.

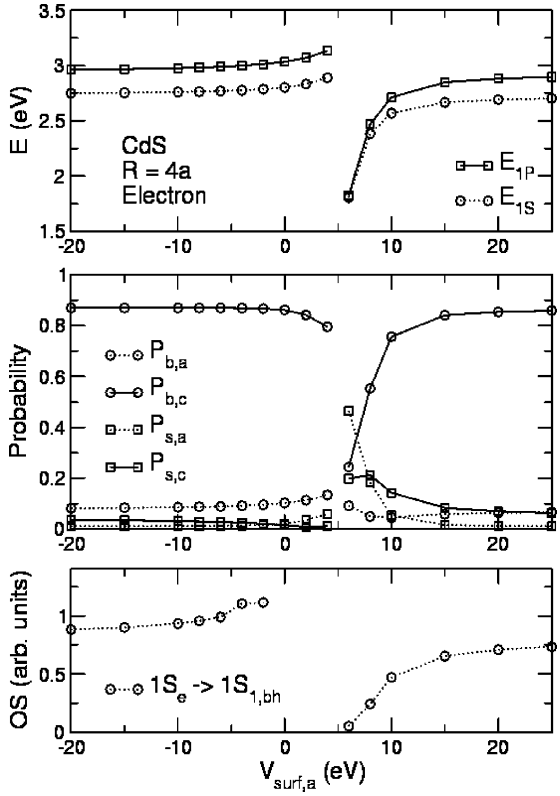

Figure 2. Dependence of the lowest electron states on the S dangling-bond energy for a $R = 4a$ CdS spherical nanocrystal with fully passivated Cd dangling bonds: energy of the lowest two electron states (top panel); probability for the 1S state to be in the bulk (b) or surface (s) on the anion (a) or cation (c) sites (middle panel); and the oscillator strength OS for the lowest active transition between the 1S electron state and an internal hole state (bottom panel).

The energy shift of the lowest two internal electron levels, the 1S and 1P states, is shown in Figure 2. In the limit of large $V_{surf,a}$, the levels approach the energies of a nanocrystal with no surface states in the gap. As $V_{surf,a}$ is reduced and the S dangling bonds become partially passivated, the S surface states are pulled down toward the gap. Level repulsion pushes the internal states steeply down below the bulk conduction band edge at 2.5 eV. At that point the surface states cross in energy the internal states (any break in the curves in Figures 2 and 3 correspond to regions where the states cannot be clearly identified as either internal or surface states). Further reduction of $V_{surf,a}$ pushes the surface states below the internal electron levels, and level repulsion between the surface states and the internal electron levels pushes the electron levels above the limit for the fully passivated surface. The upward level repulsion for $V_{surf,a} < 5$ eV is weaker than the downward level repulsion for $V_{surf,a} > 5$ eV, because level repulsion of the lower internal levels by the higher internal levels is compensated by the repulsion with the surface states when $V_{surf,a} < 5$ eV. The splitting between 1S and 1P levels is drastically reduced by the level repulsion for $V_{surf,a} > 5$ eV, because both 1S and 1P states are mixed with the surface states. For $V_{surf,a} < 5$ eV, the 1S−1P splitting is less sensitive to the repulsion by the surface states because it is compensated by level repulsion with higher states.

The energy shift of the lowest hole states is shown in Figure 3. When all dangling bonds are fully passivated, the $1P_1$ hole state has the lowest energy, and the splitting between the $1P_1$

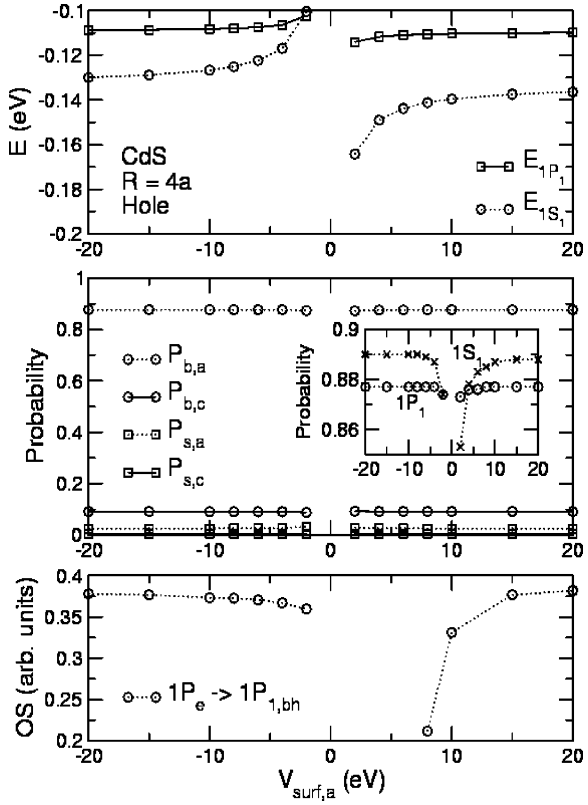

Figure 3. Dependence of the lowest hole states on the S dangling-bond energy for a $R = 4a$ CdS spherical nanocrystal with fully passivated Cd dangling bonds: energy of the lowest two hole states; probability for the $1P_1$ state to be in the bulk (b) or surface (s) on the anion (a) or cation (c) sites, the inset compares $P_{b,a}$ for the $1P_1$ and $1S_1$ hole states; and the oscillator strength OS for the lowest active transition between the $1P_1$ hole state and an internal electron state.

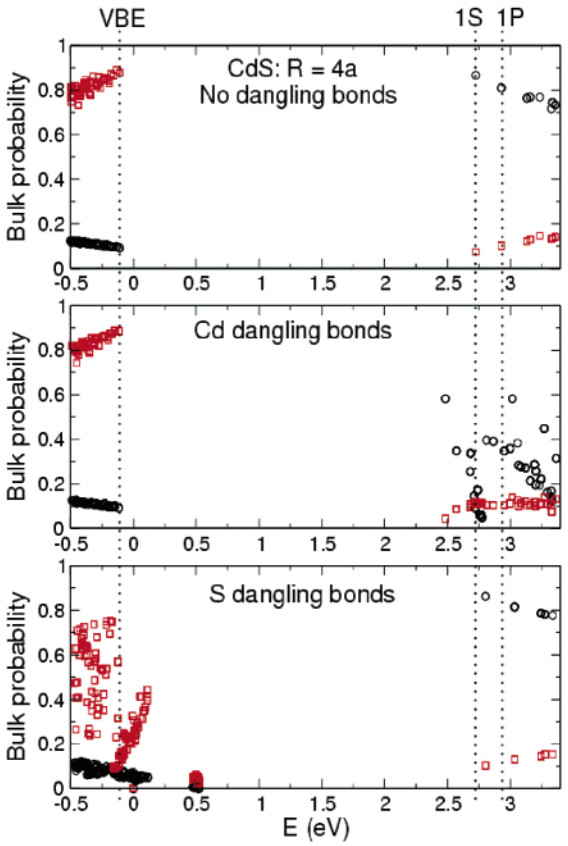

Figure 4. Probability that states in a CdS nanocrystal ($R = 4a$) with energy E occupy bulk cation (dark circles) and bulk anion (light squares) sites. Surfaces with no unpassivated dangling bonds, only Cd unpassivated dangling bonds, and only S unpassivated dangling bonds are considered. The valence band edge and the energies of the 1S and 1P electron states in the fully passivated nanocrystal are indicated.

state and the next hole state, the $1S_1$ state is about 20 meV. This level ordering and the size of the level splitting is consistent with the observation of 20 meV Stokes shifts in CdS nanocrystals of this size.[43] These levels shift significantly when the surface states cross the internal states. However, the level repulsion for hole states occurs for a narrower range of $V_{surf,a}$ than for electron states, because the internal hole states have a lower probability than the lowest electron states to be on the surface. Our results show that the $1P_1-1S_1$ splitting is insensitive to $V_{surf,a}$, except close to the limit of unpassivated S dangling bonds. Strong level repulsion for $V_{surf,a} < 0$ affects mostly the spherical $1S_1$ level and leads to a reduction of the Stokes shift and level reordering.

The probability that the 1S electron level is in the bulk or on the surface is shown in the middle panel of Figure 2. When the surface states become mixed with the internal states, the internal electron states acquire a large probability to be on S dangling bonds, even though they are electron states. The occupation probabilities show a strong dependence on dangling-bond energy when $V_{surf,a} > 5$ eV and the level repulsion by surface states is not compensated by level repulsion by higher internal states. The occupation probabilities for the $1P_1$ hole state are shown in Figure 3. As with the energy levels, the occupation probabilities for the hole states are sensitive to dangling-bond energy for a narrow rangle of $V_{surf,a}$. As the inset shows, the $1S_1$ hole state is more sensitive than the $1P_1$ state to mixing with the surface states, consistent with the reordering of the energy levels.

Finally, the oscillator strength for the lowest optically active transition from the 1S electron level is shown in the lower panel of Figure 2, and the corresponding transition from the $1P_1$ hole state is shown in Figure 3. For $V_{surf,a} > 5$ eV, the mixing of the 1S electron level with the surface states leads to a suppression of the transition rate. For $V_{surf,a} < -1$ eV, the transition rate is actually larger than in the limit of full passivation In this regime, the electron and hole states are both effected by the level repulsion with the gap states. Transitions to the $1P_1$ hole state are suppressed by any partial passivation of the S dangling bonds.

C. Uncapped Nanocrystals: Distribution of States and Optical Spectra. The distributions of states for an uncapped CdS nanocrystal ($R = 4a$) are shown in Figure 4. Fully passivated dots with all dangling bonds saturated have no surface states in the fundamental band gap, and all near-band-edge states are quantum-confined internal states. The band-edge hole states have a probability of a few percent to be on the surface. Band-edge electron states (with a lighter mass and higher kinetic energy than the holes) can penetrate to the surface more easily than holes. Thus, electrons can have a 10 percent probability to be on the surface. For large dots, the probability to be on the surface becomes negligible. For smaller dots with $R = 2a$, the probability for electrons to be on the surface can reach 25%, and for holes it can reach nearly 20%. When only the Cd dangling bonds are unpassivated, the electron states near the band edge have a significant probability to be on the surface, while the band-edge hole states are nearly identical to the hole states of the fully passivated dot. When only the S dangling bonds are unpassivated, both the electron and hole states are affected. Three distinct types of hole states occur. A narrow band of states, strongly localized to the surface dangling bonds, is in the gap at 0.5 eV. There is a second band of hole states,

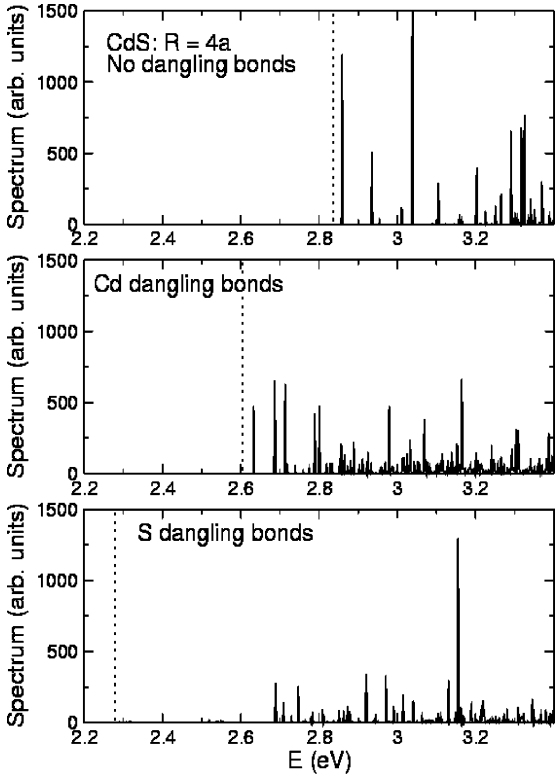

Figure 5. Optical spectra for CdS nanocrystals with radius $R = 4a$. Surfaces with no unpassivated dangling bonds, only Cd unpassivated dangling bonds, and only S unpassivated dangling bonds are considered. The position of the lowest dark transition is indicated by a dashed line in each case.

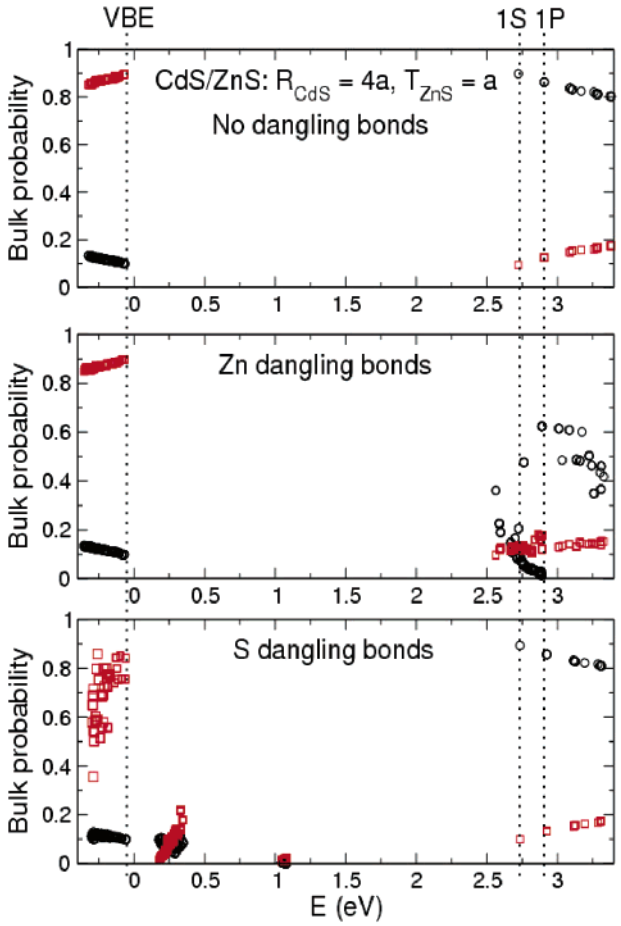

Figure 6. Probability that states in a CdS/ZnS nanocrystal (CdS core radius $R = 4a$ and ZnS shell thickness $T = a$) with energy E occupy the bulk cation (dark circles) and bulk anion (light squares) sites. Surfaces with no unpassivated dangling bonds, only Zn unpassivated dangling bonds, and only S unpassivated dangling bonds are considered. The valence band edge and the energies of the 1S and 1P electron states in the fully passivated nanocrystal are indicated.

just above the valence band edge of the fully passivated nanocrystal. These states are also significantly localized to the surface, but they also have a substantial probability to be in the bulk. Finally, hole states below the valence band edge of the passivated nanocrystal are mostly internally confined, but they still have a significant component on the surface. The electron states remain internal confined sates, but they are shifted to higher energy by level repulsion with the surface states localized on the S dangling bonds.

The corresponding optical spectra are shown in Figure 5. For the three types of surface passivation, the lowest transition is optically dark, because the lowest hole state is a $1P_0$ state that does not couple to the lowest electron state (a 1S state). The lowest transition for the fully passivated dot occurs well above the bulk band edge, as expected for quantum-confined internal states. However, when the Cd dangling bonds are unpassivated, the optically allowed transitions extend nearly 200 eV to lower energies, almost to the bulk band gap at 2.5 eV. When S dangling bonds are unpassivated, additional, optically weak transitions to the narrow surface state band at 0.5 eV and the broader surface state band just above the valence band edge occur near 2.3 and 2.5 eV, respectively. Effectively, these are deep non/weakly radiative traps. When dangling bonds are present, no transitions can be easily identified as corresponding to the dominant transitions in the fully passivated nanocrystal.

D. Capped Nanocrystals: Distribution of States and Optical Spectra. The effects of surface states on the internal confined states can be eliminated by passivating the dangling bonds. These effects can also be eliminated by separating spatially the surface and internal states by capping the quantum dot with a higher band gap shell. We consider spherical CdS nanocrystals capped with a spherical ZnS shell to determine how the capping layer affects the internal states and how thick the shell must be to eliminate the effects of the surface states. We consider three ways that the ZnS surface of a CdS/ZnS core/shell dot might be passivated: all dangling bonds passivated, only passivated Zn dangling bonds, and only passivated S dangling bonds. CdS and ZnS have a large lattice mismatch. Typically, only a few monolayers of ZnS can be grown as a capping layer before misfit dislocations occur and the optical response is degraded.[15,44] Here, we consider structures large enough that including such effects would be difficult. For these calculations, we only consider ideal, unrelaxed lattices for the capped nanocrystals. We use the same model previously used to explain the observed electronic structure of CdS/ZnS quantum-dot quantum-wells.[29]

The states for a CdS/ZnS nanocrystal with a two monolayer (ML) capping shell (CdS core radius $R = 4a$, ZnS shell thickness $T = a$, here a monolayer is taken to have a thickness of $a/2$) are shown in Figure 6. For these calculations, two-thirds of the CdS/ZnS band offset is assigned to the conduction band. Electron states weakly tunnel into the ZnS shell when the surface is fully passivated and there are no surface states to tunnel to. The lowest electron states red-shift by 1−10 meV due to the weakened confinement in the capped dot. The lowest hole states are affected more by the weaker confinement in the capped dot, red-shifting by 40−60 meV, because the barrier provided by the valence band offset is only half of the conduction band offset. As happens for the uncapped CdS dot, the lowest hole

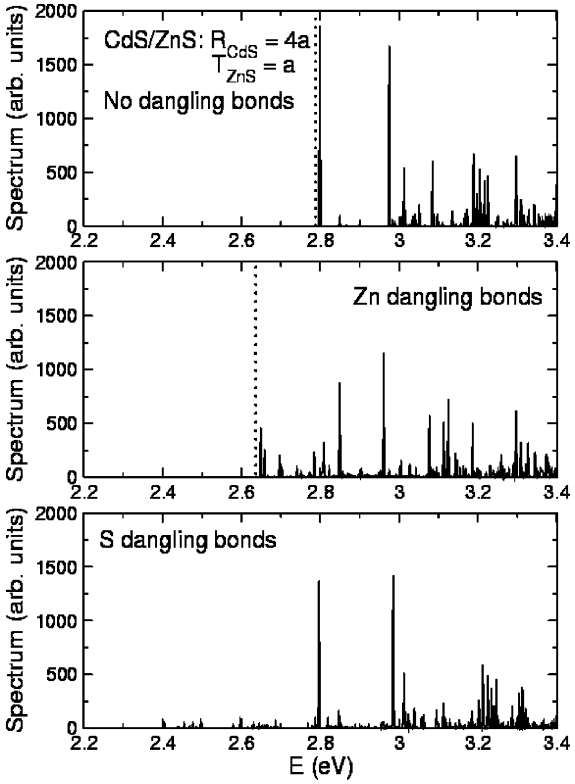

Figure 7. Optical spectrum for a CdS/ZnS nanocrystal (CdS core radius $R = 4a$ and ZnS shell thickness $T = a$). Surfaces with no unpassivated dangling bonds, only Zn unpassivated dangling bonds, and only S unpassivated dangling bonds are considered. The position of the lowest dark transition is indicated by a dashed line in each case.

states in CdS/ZnS do not shift when the surface cation dangling bonds are not passivated. When the ZnS cap provides a tunnel barrier, the lowest electron states do not shift when the surface anion dangling bonds are not passivated. In contrast, for the bare CdS dot, the lowest electron states are blue-shifted by level repulsion with surface states provided by unpassivated anion dangling bonds. However, internal electron states are still significantly perturbed by unpassivated cation dangling bonds, and internal hole states are significantly perturbed by unpassivated anion dangling bonds even when the CdS is capped with 2 ML of ZnS. No low-energy electron states can be clearly identified as an internal confined state when there are unpassivated cation dangling bonds (although the probability to be in the bulk is higher than for the uncapped dot). When the surface S dangling bonds are unpassivated, two bands of surface states are present, as for the uncapped dot. However, when the capping is added, these states are more completely confined to the surface. Conversely, lower-energy hole states are more strongly localized to the interior when the capping is added.

The spectra of CdS dots with a 2-ML ZnS cap for the three surface passivations are shown in Figure 7. A Stokes shift is still observed in each case, indicating that the lowest transition remains dark when a thin capping shell is added. When the Zn dangling bonds are unpassivated, no transitions can be identified with those transitions between internal confined states that are dominant for the fully passivated dot. Moreover, those transitions close to the bulk band edge that involve surface states remain significant when the 2-ML cap is added. However, when S surface dangling bonds are unpassivated, the transitions to the localized hole surface state bands are significantly weakened when the 2-ML ZnS barrier is added. In this case, the two dominant lowest transitions involving internal confined states can be identified.

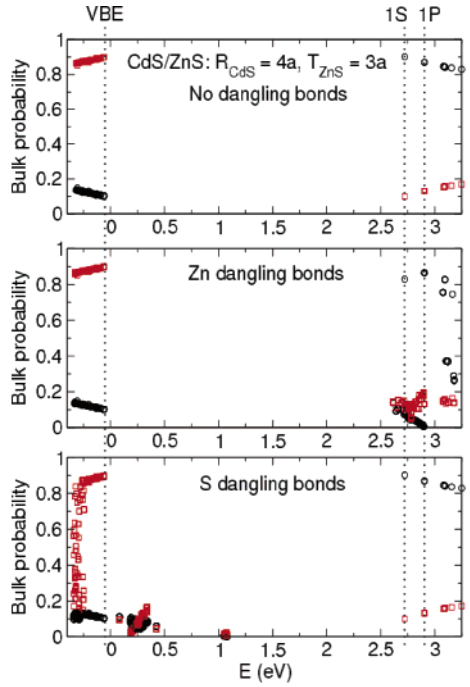

Figure 8. Probability that states in a CdS/ZnS nanocrystal (CdS core radius $R = 4a$ and ZnS shell thickness $T = 3a$) with energy E occupy the bulk cation (dark circles) and bulk anion (light squares) sites. Surfaces with no unpassivated dangling bonds, only Zn unpassivated dangling bonds, and only S unpassivated dangling bonds are considered. The valence band edge and the energies of the 1S and 1P electron states in the fully passivated nanocrystal are indicated.

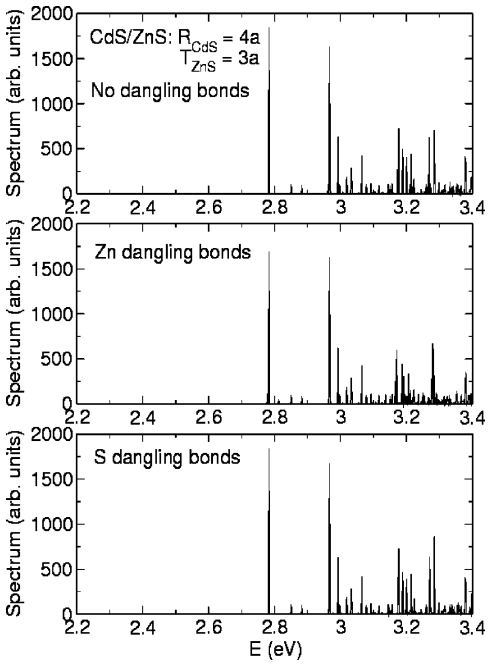

Figure 9. Optical spectrum for a CdS/ZnS nanocrystal (CdS core radius $R = 4a$ and ZnS shell thickness $T = 3a$). Surfaces with no unpassivated dangling bonds, only Zn unpassivated dangling bonds, and only S unpassivated dangling bonds are considered. The lowest transition is optically active in each case.

Thicker caps are needed to fully eliminate the effects of surface states on the internal confined states. The distribution of states and the spectra are shown in Figures 8 and 9 for CdS dots capped with 6 ML of ZnS ($T = 3a$). Clearly defined internal confined electron and hole states can be seen for each surface passivation. The energies of the lowest confined states are independent of the passivation. The distinction between surface

and internal confined states is clearer. In fact, a narrow band of states in the valence band is obviously another band of states that can strongly hybridize with surface states. This band occurs at the ZnS valence band edge and results from states that can propagate freely to the surface above the ZnS barrier. This band is not obvious for thinner caps.

For thick caps, the spectra are insensitive to the surface passivation. The same dominant transitions involving internal confined states are seen for each surface passivation considered here. Transitions to surface states do not have any substantial oscillator strength, although the surface states would still provide dark traps if tunneling to the surface is possible. For thicker shells, the Stokes shift disappears, and the lowest transition involving internal states is optically active because the 1S hole state becomes the hole ground state. The order of the 1S and 1P hole states is reversed for thick caps because the spherically symmetric 1S hole state is more strongly red-shifted than the 1P state by the weaker confinement of a thick cap.

4. Conclusions

We have used a tight-binding approach to study the effect of surface states on capped and uncapped nanocrystals. We consider ideal nanocrystals with unrelaxed surfaces and ignore the effects of lattice mismatch in capped structures. We consider CdS and CdS/ZnS dots. An atomistic approach is necessary to correctly account for the effect of the surface, even in the limit when all of the surface dangling bonds are passivated. Internal confined states can have a substantial probability to be on the dot surface. Atomistic models are needed to account for this. Effective mass models can only account for this if an effective dot size, bigger than the dot physical size, is used. The surface passivation has a critical effect on the low-energy states. We consider a simple model in which the passivation is modeled as an energy shift of the dangling bonds. The shift of the low-energy states due to passivation can be as large as the shift due to confinement. Confined states can even be pushed below the bulk band edge by the passivation. When surface anion dangling bonds are unpassivated, an anion-derived, narrow (bandwidth 0.05 eV), surface-state band lies 0.5 eV above the valence band edge and a broader (0.2 eV) band of back-bonded surface states exists in the gap just above the valence band edge. These bands are narrow because the hole mass is heavy. When surface cation dangling bonds are unpassivated, a broad band of mixed surface/internal states exists above the conduction band edge. The mixing is large because the electron mass is light. Experiments done on single nanocrystals could distinguish between these types of surface states. The effects of the surface states can be eliminated by capping the dot with a higher band gap shell. When a few monolayer cap is used, the effect of surface states is still significant. A six-monolayer cap is needed to fully suppress the effects of surface states on the internally confined states in an ideal CdS/ZnS capped nanocrystal. Careful growth of the cap will be needed to produce thick enough caps without defects so that the maximum quantum yield can be achieved.

Acknowledgment. Support from projects KBN-3T1104326 and PZB-MIN-008/P03/2003 is gratefully acknowledged.

References and Notes

(1) Bruchez, M., Jr.; Moronne, M.; Gin, P.; Weiss, S.; Alivisatos, A. P. *Science* **1998**, *281*, 2013.

(2) Chan, W. C. W.; Nie, S. *Science* **1998**, *281*, 2016.

(3) Dubertret, B.; Skourides, P.; Norris, D. P.; Noireaux, V.; Brivanlou, A. H.; Libchaber, A. *Science* **2002**, *298*, 1759.

(4) Larson, D. R.; Zipfel, W. R.; Williams, R. M.; Clark, S. W.; Bruchez, M. P.; Wise, F. W.; Webb, W. W. *Science* **2003**, *300*, 1434.

(5) Willard, D. M.; Carillo, L. L.; Jung, J.; Van Orden, A. *Nano Lett.* **2001**, *1*, 469.

(6) Mamedova, N. N.; Kotov, N. A.; Rogach, A. L.; Studer, J. *Nano Lett.* **2001**, *1*, 281.

(7) Medintz, I. L.; Clapp, A. R.; Mattoussi, H.; Goldman, E. R.; Fisher, B.; Mauro, J. M. *Nat. Mater.* **2003**, *2*, 630.

(8) Ouyang, M.; Awschalom, D. D. *Science* **2003**, *301*, 1074.

(9) Dollefeld, H.; Weller, H.; Eychmuller, A. *Nano Lett.* **2001**, *1*, 267.

(10) Sirota, M.; Minkin, E.; Lifshitz, E.; Hensel, V.; Lahav, M. *J. Phys. Chem. B* **2001**, *105*, 6792.

(11) Torimoto, T.; Yamashita, M.; Kuwabata, S.; Sakata, T.; Mori, H.; Yoneyama, H. *J. Phys. Chem. B* **1999**, *103*, 8799.

(12) Ding, S.-Y.; Jones, M.; Tucker, M. P.; Nedeljkovic, J. M.; Wall, J.; Simon, M. N.; Rumbles, G.; Himmel, M. E. *Nano Lett.* **2003**, *3*, 1581.

(13) Kortan, A. R.; Hull, R.; Opila, R. L.; Bawendi, M.; Steigerwald, M. L.; Carroll, P. J.; Brus, L. E. *J. Am. Chem. Soc.* **1990**, *112*, 1327.

(14) Peng, X.; Schlamp, M. C.; Kadavanich, A. V.; Alivisatos, A. P. *J. Am. Chem. Soc.* **1997**, *119*, 7019.

(15) Dabbousi, B. O.; Rodriguez-Viejo, J.; Mikulec, F. V.; Heine, J. R.; Mattoussi, H.; Ober, R.; Jensen, H. F.; Bawendi, M. G. *J. Phys. Chem. B* **1997**, *101*, 9463.

(16) Cao, Y. W.; Banin, U. *J. Am. Chem. Soc.* **2000**, *122*, 9692.

(17) Lu, S.-Y.; Wu, M.-L.; Chen, H.-L. *J. Appl. Phys.* **2003**, *93*, 5789.

(18) Hohng, S.; Ha, T. *J. Am. Chem. Soc.* **2004**, *126*, 1324.

(19) Efros, Al. L.; Rosen, M.; Kuno, M.; Nirmal, M.; Norris, D. J.; Bawendi, M. G. *Phys. Rev. B* **1996**, *54*, 4843.

(20) Banin, U.; Lee, J. C.; Guzelian, A. A.; Kadavanich, A. V.; Alivisatos, A. P.; Jaskolski, W.; Bryant, G. W.; Efros, Al. L.; Rosen, M. *J. Chem. Phys.* **1998**, *109*, 2306.

(21) Efros, Al. L.; Rosen, M. *Phys. Rev. B* **1998**, *58*, 7120.

(22) Li, J.; Xia, J.-B. *Phys. Rev. B* **2000**, *62*, 12613.

(23) Fonoberov, V. A.; Pokatilov, E. P.; Balandin, A. A. *Phys. Rev. B* **2002**, *66*, 85310.

(24) Wang, L. W.; Zunger, A. *Phys. Rev. B* **1996**, *53*, 9579.

(25) Lippens, P. E.; Lannoo, M. *Phys. Rev. B* **1989**, *39*, 10935.

(26) Ramaniah, L. M.; Nair, S. V. *Phys. Rev. B* **1993**, *47*, 7132.

(27) Leung, K.; Whaley, K. B. *Phys. Rev. B* **1997**, *56*, 7455.

(28) Leung, K.; Pokrant, S.; Whaley, K. B. *Phys. Rev. B* **1998**, *57*, 12291.

(29) Little, R. B.; El-Sayed, M. A.; Bryant, G. W.; Burke, S. E. *J. Chem. Phys.* **2001**, *114*, 1813.

(30) Bryant, G. W.; Jaskolski, W. *Phys. Rev. B* **2003**, *67*, 205320.

(31) Perez-Conde, J.; Bhattacharjee, A. K. *Phys. Rev. B* **2003**, *67*, 235303.

(32) Braginsky, L. S. *Phys. Rev. B* **1999**, *60*, 13970; Rodina, A. V.; Alekseev, A. Yu.; Efros, Al. L.; Rosen, M.; Meyer, B. K. *Phys. Rev. B* **2002**, *65*, 125302.

(33) Hill, N. A.; Whaley, K. B. *J. Chem. Phys.* **1994**, *100*, 2831.

(34) Leung, K.; Whaley, K. B. *J. Chem. Phys.* **1999**, *110*, 11012.

(35) Pokrant, S.; Whaley, K. B. *Eur. Phys. J. D* **1999**, *6*, 255.

(36) Puzder, A.; Williamson, A. J.; Reboredo, F. A.; Galli, G. *Phys. Rev. Lett.* **2003**, *91*, 157405.

(37) Puzder, A.; Williamson, A. J.; Zaitseva, N.; Galli, G.; Manna, L.; Alivisatos, A. P. *Nano Lett.* **2004**, *4*, 2361.

(38) Vogl, P.; Hjalmarson, H. P.; Dow, J. D. *J. Phys. Chem. Solids* **1983**, *44*, 365.

(39) Madelung, O., Schulz, M., Weiss, H., Eds.; *Landolt-Börnstein, Numerical Data and Functional Relationships in Science and Technology*, Group III, Volume 17, Springer-Verlag: Berlin, 1982.

(40) Lee, S.; Oyafuso, F.; von Allmen, P.; Klimeck, G. *Phys. Rev. B* **2004**, *69*, 45316.

(41) Frage, S.; Muszynska, J. *Atoms in External Fields*; Elsevier: New York, 1981.

(42) Lee, S.; Jonsson, L.; Wilkins, J. W.; Bryant, G. W.; Klimeck, G. *Phys. Rev. B* **2001**, *63*, 195318.

(43) Yu, Z.; Li, J.; O'Connor, D. B.; Wang, L.-W.; Barbara, P. F. *J. Phys. Chem. B* **2003**, *107*, 5670.

(44) Talapin, D. V.; Mekis, I.; Gotzinger, S.; Kornowski, A.; Benson, O.; Weller, H. *J. Phys. Chem B* **2004**, *108*, 18826.